

Supersonic turbulence and structure of interstellar molecular clouds

Stanislav Boldyrev

Institute for Theoretical Physics, Santa Barbara, California 93106, boldyrev@itp.ucsb.edu

Åke Nordlund

Copenhagen Astronomical Observatory and Theoretical Astrophysics Center, DK-2100 Copenhagen, Denmark, aake@astro.ku.dk

Paolo Padoan

*Jet Propulsion Laboratory, 4800 Oak Grove Drive, MS 169-506,
California Institute of Technology, Pasadena, CA 91109-8099, padoan@jpl.nasa.gov
(March 25, 2002)*

The interstellar medium (ISM) provides a unique laboratory for highly supersonic, driven hydrodynamics turbulence. We present a theory of such turbulence, confirm it by numerical simulations, and use the results to explain observational properties of interstellar molecular clouds, the regions where stars are born.

1. Introduction. Stars are formed as a result of gravitation (Jeans) collapse of dense clumps in interstellar molecular clouds. The structure of such clouds in a large interval of scales (from about $100pc$ to $0.01pc$) lacks any characteristic length, and can be understood as arising from supersonic hydrodynamic motions sustained on large scales by supernovae explosions [11,1,19]. A fluid motion with characteristic large-scale relative velocities of order 1-10 km/sec compresses rapidly radiating and therefore relatively cold molecular gas ($T \sim 10K$) up to very high densities (above $10^4 cm^{-3}$). Instabilities of shock fronts create a hierarchy of gas clumps with broad mass, size, and velocity distribution controlled by the Mach number ($M = v/c$) and by the Alfvénic Mach number ($M_a = v/v_a$), where v_a is the Alfvén velocity, $v_a = B/\sqrt{4\pi\rho}$, and c is the sound speed. Depending on parameters of clouds, the Mach number can be about 30 on the largest scales, and the Alfvénic Mach number can exceed 1 as well [20,21,13,14,22,28,25,26]. A systematic study of scaling properties of supersonic turbulence and of the structure of molecular clouds was initiated by the work of Larson [20,21], but despite the large number of observational and numerical investigations that appeared for the last 20 years, the theoretical understanding of the turbulence has been rather poor.

In the present paper we provide a new analytical model for a supersonic turbulent cascade and test the model against observations and numerical simulations. We find a very good agreement within the error bar uncertainty. The analytical approach is suggested by the following two numerical results. First of all, we establish that for large Mach numbers ($M > 2$) the velocity field in the inertial interval is mostly divergence-free and shear-dominated, with the intensity of its potential component being only about 10% of the intensity of its solenoidal part. The second finding is that the most intense dissipative structures of the turbulence are two-dimensional sheets or shocks

as oppose to the incompressible case where most of energy is dissipated in filaments, see also [26,33]. Using these two ingredients in the framework of the so-called She-Lévêque model of turbulence we calculate two-point correlators of velocity and density fields. This allows us to construct the multifractal distributions of velocity and density fields, that statistically describe the structure of a turbulent molecular cloud. In the present paper we present the analytic derivation of the model and summarize the most important numerical results. The detailed numerical and observational analysis will appear elsewhere [4,27].

In the following section we construct the multifractal distribution of the velocity field, and numerically check the first 10 velocity-difference structure functions [the definition is given below]. In section 3 we proceed with the density distribution, derive a general formula for two-point density correlators and compare the result with the numerical simulations. Conclusions, applications, and future research are outlined in section 4.

2. Multifractal model of supersonic turbulence. In 1994 She and Lévêque suggested a model that turned out to be very successful in explaining the experimental findings for incompressible turbulence [34]. The model represents a turbulent cascade as an infinitely-divisible log-Poisson process [9,35,24], and has three input parameters. The first two of them are the so-called *naïve*, i.e., non-intermittent, scaling exponents of velocity fluctuation and of the eddy turnover time. The non-intermittent velocity of the eddy of size l scales as $v_l \sim l^\Theta$, and the “eddy turnover” time scales as $t_l \sim l^\Delta$. The third parameter is the dimension of the most intense dissipative structure, D . In the incompressible case, the first two parameters take their Kolmogorov values, $\Delta = 2/3$, $\Theta = 1/3$, and the third parameter is $D = 1$ since the dissipation mostly occurs in elongated filaments.

The model predicts the so-called structure functions of

the velocity field that are defined as follows

$$S_n(l) = \langle |v(x+l) - v(x)| \rangle \sim l^{\zeta(n)}. \quad (1)$$

The velocity components in this formula can be either parallel or perpendicular to vector l . In the former case the structure function is called longitudinal, in the latter case transversal. There is experimental evidence that both scale in the same way [2,6,15], therefore, we will not distinguish between them as far as the scaling is concerned. The She-L  v  que formula gives the following expression for the scaling exponents of the structure functions,

$$\zeta(n) = \Theta(1 - \Delta)n + (3 - D)(1 - \Sigma^{\Theta n}), \quad (2)$$

where $\Sigma = 1 - \Delta/(3 - D)$ [34]. This expression has been experimentally checked to work for structure functions up to the 10th order, within an accuracy of a few percent [2,34].

To address the *supersonic* case, we note that in the inertial interval the turbulence is still mostly divergence-free (Fig. (1)). The effect of vorticity generation in the random 3D flow is analogous to the effect of magnetic dynamo, since magnetic field and vorticity obey the same dynamic equation. We therefore leave the Kolmogorov parameters Θ and Δ unchanged.

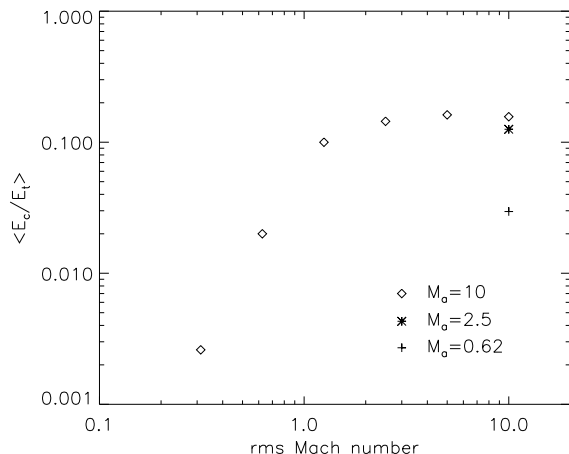


FIG. 1. Results from numerical simulations of randomly driven MHD equations with resolution 128^3 . The ratios of the potential, E_c , to the solenoidal, E_t , part of the velocity field are presented for the Mach numbers up to $M = 10$ at the largest scale. The initial magnetic Mach number has been chosen in the range $M_a = 0.6, \dots, 10$, and the numerical integration has been conducted for several turn-over times of the largest eddies, which was enough to reach the steady state. The isothermal equation of state was used and the large-scale driving force was Gaussian, solenoidal, and correlated at a turn-over time of the largest eddy. The detailed description of the numerical set up can be found in [4]. The scaling relations reported in the present paper were obtained for $M \simeq 10$, and $M_a \simeq 3$.

However, the most dissipative structures of a supersonic flow are different from the incompressible case. Instead of filaments they look like shocks or two-dimensional dissipative sheets, therefore, $D = 2$ [3,4]. With such input parameters, formula (2) is recast as

$$\zeta(n) = n/9 + 1 - (1/3)^{n/3}. \quad (3)$$

Quite remarkably, this formula works with good accuracy for the numerical simulations, fitting the first ten structure functions with an error of about 5%, see Fig.(2).

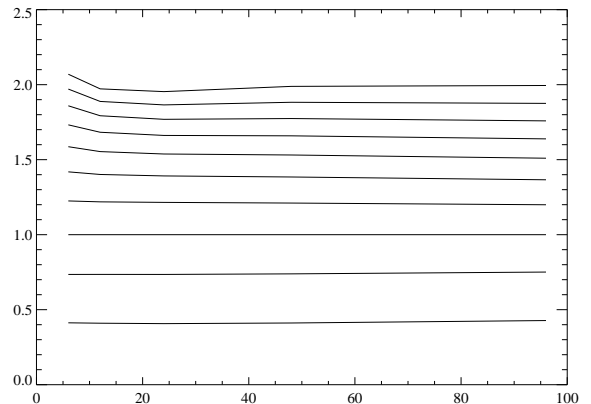


FIG. 2. Slopes of transversal structure functions computed for $n = 1, 2, \dots, 10$ (correspondingly, from bottom to top), in the 250^3 run with $M = 10$ and $M_a = 3$. The plot presents the ratios of the *differential* slopes of the structure functions to the differential slope of $S_3(l)$. These ratios, $\zeta(n)/\zeta(3)$, exhibit excellent scalings, in agreement with the Extended Self-Similarity hypothesis [2]. They are well described by our formula (3). Note the strong difference of the scalings of the structure functions from the scalings given by the Kolmogorov model, $\zeta(n) = n/3$, and by the Burgers model, $\zeta(n) = 1$, see [15].

The observational data consistently indicate steeper than Kolmogorov velocity spectra, see e.g. [25,14]. Our model (3) predicts $|v_k|^2 \sim k^{-1-\zeta(2)} = k^{-1.74}$, which agrees with observations within error bars. Interestingly enough, the average velocity spectrum, originally inferred from observations by Larson, was $k^{-1.74}$ on scales of order $1pc < l < 1000pc$, and $k^{-1.76}$ towards smaller scales, $0.1pc < l < 100pc$ [21,20].

On the analytical side, the model (3) implies the so-called multi-fractal distribution of the turbulent fluctuations. Here we discuss the statistics of the velocity field, and in the next section, apply the results to the density field. To visualize the model, assume that the whole space (a molecular cloud or a simulation domain) contains turbulent structures of different (in general, fractal) dimensions. In the vicinity of a particular structure, the velocity difference scales with some particular exponent that we denote by h , i.e., $v_l \sim l^h$. The dimension of this fractal structure will be denoted $D(h)$. If we divide the

space into small boxes of size l , then the number of boxes covering the fractal structure of dimension D is proportional to l^{-D} , while the total number of boxes is proportional to l^{-3} . The probability to find ourselves inside a box covering the fractal with dimension $D(h)$ is therefore $p_h(l) \sim l^{3-D(h)}$. To average the n 's moment of the velocity difference we just need to sum $l^{nh}p_h(l)$, which is the contribution of one particular fractal structure, over all the fractal structures. We get

$$S_n(l) \sim \sum_h l^{nh+3-D(h)} \sim l^{\zeta(n)}. \quad (4)$$

Knowing $D(h)$ is equivalent to knowing $\zeta(n)$, these two functions are related by the Legendre transform as one immediately gets by assuming that l is small, and by evaluating the sum in (4) by the steepest descent method [15]. For example, knowing $\zeta(n)$ from (3), one can restore $D(h)$; we, however, will not need $D(h)$ for our present purposes.

3. Multifractal distribution of the density field. First we would like to derive an important relation of supersonic turbulence. We start with the Navier-Stokes and continuity equations:

$$\partial_t \mathbf{u} + (\mathbf{u} \cdot \nabla) \mathbf{u} = (\eta/\rho) \Delta \mathbf{u} - c^2 \nabla \rho / \rho + \mathbf{f}, \quad (5)$$

$$\partial_t \rho + \nabla \cdot (\rho \mathbf{u}) = 0. \quad (6)$$

Let us introduce the density correlator $R(t, x) = \langle \rho(x_1, t) \rho(x_2, t) \rangle$, and the density-weighted second-order velocity structure function, $G^{ik}(t, x) = \langle \rho(1) \rho(2) [u(1) - u(2)]^i [u(1) - u(2)]^k \rangle$, where $\mathbf{x} = \mathbf{x}_1 - \mathbf{x}_2$. Averaging is performed over the random force. Differentiating $R(t, x)$ with respect to time, and using (5) and (6), one gets:

$$\begin{aligned} \partial_t^2 R + \nabla_i \nabla_k G^{ik} - c^2 \Delta R + \nabla_i \langle [f(1) - f(2)]^i \rho(1) \rho(2) \rangle \\ = 2\eta \Delta \nabla_i \langle u(1)^i \rho(2) \rangle, \end{aligned} \quad (7)$$

where the spatial derivatives are taken with respect to \mathbf{x} . In the inertial interval, the forcing and the viscous terms are small. In the supersonic regime, one can also neglect the c^2 term. Assuming now that the turbulence is in a steady state, we are left with a simple equation that must hold in the inertial interval, $\nabla_i \nabla_k G^{ik} = 0$. Due to spatial isotropy we get:

$$G^{ik}(x) = A \delta^{ik} + O(x^2/L^2) + \dots, \quad (8)$$

where L is the external force correlation length, and A is some constant. In the inertial interval, $x \ll L$, one gets $G = \text{const.}$ To obtain the density distribution let us make a natural assumption that both the density and the velocity fields have fixed scalings in the vicinity of the *same* turbulent structures. In other words, close to a fractal structure where the velocity field has scaling h , the density field has some other, but also constant along the same structure, scaling $\alpha(h)$, i.e., $\rho(l) \sim l^{\alpha(h)}$. The condition (8) now reads

$$G \sim \sum_h l^{2h+2\alpha(h)+3-D(h)} = \text{const.} \quad (9)$$

The other restriction comes from the mass conservation law,

$$\langle \rho \rangle \sim \sum_h l^{\alpha(h)+3-D(h)} = \text{const.} \quad (10)$$

Strictly speaking, our constraint conditions (9) and (10) are to a certain extent phenomenological. However, we found them to be consistent with our simulations. Moreover, the theory based on them predicts density correlators rather successfully, which we are going to demonstrate now. Let us assume that the function $\alpha(h)$ is analytic and can be expanded as $\alpha(h) = a + bh + gh^2 + \dots$. As a minimal model, consider the case, when $\alpha(h)$ is a *linear* function, $\alpha(h) = a + bh$. It turns out that such a linear ansatz is consistent with both restriction conditions (9) and (10). As follows from (4), the mass conservation condition (10) is satisfied with $a = -\zeta(p)$ and $b = p$, where p is arbitrary. The equation for p is then derived from the dynamic constraint (9), which gives $\zeta(2p + 2) = 2\zeta(p)$. The solution of this equation will be denoted as p_0 . If we use our formula (3), p_0 can be found exactly; we thus obtain $b = p_0 = 2.28$ and $a = -\zeta(p_0) = -0.82$. The multifractal distribution for the density field, $D_\rho(\alpha)$, is thus related to the multifractal distribution of the velocity field, $D_\rho(\alpha) = D[(\alpha + \zeta(p_0))/p_0]$. Fractal and multifractal distributions of density fields have indeed been inferred from observations, see, e.g., [12, 7], and from numerical simulations [8].

By analogy with the velocity field, the quantities of practical interest are density correlators. They can be calculated with the aid of a formula analogous to (4),

$$\langle [\rho(x+l)\rho(x)]^m \rangle \sim \sum_h l^{2m\alpha(h)+3-D(h)} \sim l^{\xi(m)}. \quad (11)$$

Upon substituting the linear expression for $\alpha(h)$ and using formula (4), one immediately gets $\xi(m) = \zeta(2mp_0) - 2m\zeta(p_0)$. This formula allows one to obtain the density scaling if the velocity structure functions are known either from theory or from experiment. Since $\zeta(n)$ is a concave function, $\xi(m)$ is negative for $m > 1/2$. For $m = 1, 2, 3$ the formula gives $\xi(1) \simeq -0.3$, $\xi(2) \simeq -1.3$, and $\xi(3) \simeq -2.4$, values close to what is obtained in the numerics, see Fig. (3). We give here only the first three exponents since starting from $m = 3$, the density exponents depend on velocity structure functions of order higher than 13, which cannot be reliably produced with our numerical resolution.

4. Conclusions. We have suggested a self-consistent model that provides an explanation for numerical and observational scaling laws of supersonic ISM turbulence, the so-called Larson's laws. We would like to conclude with the following remarks:

1. The She-Leveque approach was also applied to *incompressible* MHD turbulence in [18,31,23], where different scalings were suggested. Most successful was the approach of Müller and Biskamp [23], where the energy cascade was assumed to be Kolmogorov-like, but the dissipation occurred in micro current sheets. In this case, the same formula (3) gave a good agreement with numerical simulations for structure functions up to order 8. Our results together with those by Müller and Biskamp support the ideas put forward in [9] and [35], that completely different turbulent systems can belong to the same class of universality, i.e. have the same velocity scaling exponents.
2. Turbulence with small pressure is usually referred to as Burgers turbulence, the theory of which has been rapidly developing in recent years [32,37,5,10,17,36,16,30]. However, the Burgers velocity field is usually assumed to be potential, which is true in one and two dimensions, but inconsistent with the 3D case due to strong vorticity generation. However, our general relation, $\rho(1)\rho(2) \sim |v(1) - v(2)|^{2p_0}/l^{2\zeta(p_0)}$, which is valid inside any correlation function, can be useful for the closure problems of Burgers turbulence.
3. Our model is consistent with available observational results, although the error bars of observed velocity structure functions are too large for a precise comparison. Moreover, only projected quantities (i.e., integrated along the line of sight) are observationally available, and therefore the 3D results should be reformulated for these projected fields — this is a subject of future work [27].

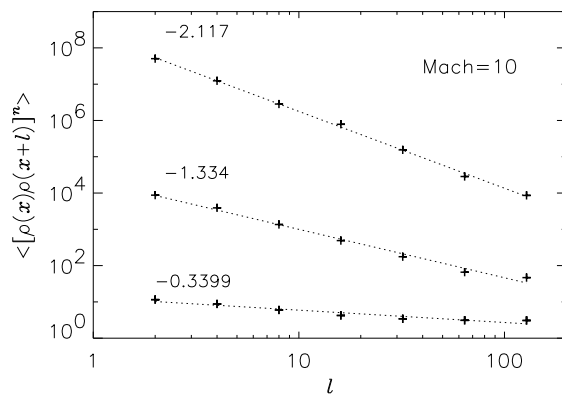


FIG. 3. Density correlators for $m = 1, 2, 3$. The numerically obtained slopes are $\xi(1) \simeq -0.3$, $\xi(2) \simeq -1.3$, and $\xi(3) \simeq -2.1$, close to the theoretical prediction (11). The numerical simulations are the same as in Fig. (1).

- [1] de Avillez, M. A. MNRAS **315** (2000) 479.
- [2] Benzi, R., Struglia, M. V., and Tripiccone, R. Phys. Rev. E **53** (1996) R5565; Benzi, R., Ciliberto, S., Tripiccone, R., Baudet, C., Massaioli, and Succi, S., Phys. Rev. E **48** (1993) R29.
- [3] Boldyrev S., ApJ **569**, No. 2, April 20 (2002) ; astro-ph/0108300.
- [4] Boldyrev, S., Nordlund, Å., and Padoan, P., ApJ **573**, No. 2(1) July 10, 2002; astro-ph/0111345.
- [5] Boldyrev, S., Phys. Rev. E **55** (1997) 6907.
- [6] Camussi, R. and Benzi, R., Phys. Fluids **9** (1997) 257.
- [7] Chappell, D. and Scalo, J., Astrophys. J. **551** (2001) 712.
- [8] Chicana-Nuncebay, W., & Vázquez-Semadeni, E., 2001, in "Computational Fluid Dynamics. Proceedings of the Fourth UNAM Supercomputing Conference", eds. E. Ramos, G. Cisneros, R. Fernandez-Flores and A. Santillan (Singapore: World Scientific), p. 96.
- [9] Dubrulle, B., Phys. Rev. Lett. **73** (1994) 959.
- [10] E, W., Khanin, K., Mazel, A., and Sinai, Ya., Phys. Rev. Lett. **78** (1997) 1904; E, W. and Vanden Eijnden, E., Phys. Rev. Lett. **83** (1999) 2572.
- [11] Elmegreen, B. G. (2001), in "From Darkness to Light", ed. T. Montmerle & P. Andre, ASP Conference Series, in press; astro-ph/0010582.
- [12] Elmegreen, B. G. and Falgarone, E., ApJ **471** (1996) 816.
- [13] Falgarone, E. and Phillips, T. G., ApJ **359** (1990) 344.
- [14] Falgarone, E., Puget, J.-L., and Perault, M. A&A **257** (1992) 715.
- [15] Frisch, U. (1995) *Turbulence* (Cambridge University Press).
- [16] Frisch, U. and Bec, J., (2000) nlin.CD/0012033.
- [17] Gotoh, T. and Kraichnan, R. H., Phys. Fluids **10** (1998) 2859.
- [18] Grauer, R., Krug, J., and Marliani, C., Phys. Lett. A **195** (1994) 335.
- [19] Korpi, M. J., Brandenburg, A., Shukurov, A., Tuominen, I., and Nordlund, Å. ApJ **514** L99.
- [20] Larson, R. B., MNRAS **186** (1979) 479.
- [21] Larson, R. B., MNRAS **194** (1981) 809.
- [22] Myers, P. C. and Gammie, C. F., ApJ **522** (1999) L141.
- [23] Müller, W.-C. and Biskamp, D., Phys. Rev. Lett. **84** (2000) 475.
- [24] Novikov, E. A., Phys. Rev. E **50** (1994) R3303.
- [25] Ossenkopf, V. and Mac Low, M.-M., (2000) astro-ph/0012247.
- [26] Ostriker, E. C., Stone, J. M., and Gammie, C. F., ApJ **546** (2001) 980.
- [27] Padoan, P., Boldyrev S., Langer, W., and Nordlund, Å., in preparation.
- [28] Padoan, P. and Nordlund, Å., ApJ **526** (1999) 279.
- [29] Padoan, P. and Nordlund, Å., (2000) astro-ph/0011465.
- [30] Passot, T. & Vázquez-Semadeni, E., Phys. Rev. E **58** (1998) 4501.
- [31] Politano, H. and Pouquet, A., Phys. Rev. E **52** (1995) 636.
- [32] Polyakov, A. Phys. Rev. E **52**, 6183 (1995).

- [33] Porter, D., Pouquet, A., Sytine, I., Woodward, P., Physica A **263** (1999) 263; Porter, D. H., Woodward, P. R., and Pouquet, A., Phys. Fluids **10** (1998) 237.
- [34] She, Z.-S. and L  v  que, E., Phys. Rev. Lett. **72** (1994) 336.
- [35] She, Z.-S. and Waymire, E. C., Phys. Rev. Lett. **74** (1995) 262.
- [36] Verma, M. K., (2000) Physica A, **277**, 359.
- [37] Yakhot, V. and Chekhlov, A., Phys. Rev. Lett. **77** (1996) 3118.